Published by :
https://www.ijert.org/
An International Peer-Reviewed Journal

International Journal of Engineering Research & Technology (IJERT)
ISSN: 2278-0181
Vol. 15 Issue 04 , April - 2026

Dynamic and Serviceability Performance of a 70 m (G+18) Reinforced Concrete Building per Indian Standards Using ETABS

Sourabh Patil
PG Student, Department of Structural Engineering, PVPIT, Budhgaon.

Prof. N. S. Patil
Department of Structural Engineering, PVPIT, Budhgaon, Maharashtra, India

Abstract - ***This paper reports the modeling assumptions, load definition, analysis setup, and response synthesis for a 70 m (G+18) reinforced concrete (RC) building analyzed in ETABS with a central RC core coupled to perimeter moment-resisting frames. The analytical workflow is aligned with Indian practice through the use of seismic action definition per IS 1893 (Part 1):2016, tall-building performance intent per IS 16700, reinforced concrete member behavior and detailing philosophy per IS 456:2000, and (where any steel components or connectors exist) design basis per IS 800:2007. Response-spectrum seismic analyses are performed in both principal directions (EQX, EQY) along with along-wind serviceability action in the X direction (WindX). P–Delta effects are enabled to capture second-order amplification and stability sensitivity. Global dynamic characteristics (fundamental periods, torsional period, modal mass participation) are summarized together with storey-wise displacement, inter-storey drift, storey shear, overturning moments, and peak floor acceleration (PFA). The results indicate a clear governance split: along-wind action governs roof displacement (about 220 mm), while seismic action governs peak inter-storey drift (about 0.357% in EQX and 0.342% in EQY), with drift peaks occurring in an upper-middle height band. Base shear and overturning actions are consistent with a core–frame system at this height (approximately 9,000 kN base shear and 267 MN·m base overturning moment in EQX). PFA increases with height and approaches about 0.12 g at the roof under seismic action, highlighting the need for non-structural acceleration-sensitive coordination. The paper concludes with targeted stiffness tuning recommendations, stability monitoring guidance, and non-structural design implications based on the extracted response set.***

Key Words: **ETABS; G+18 RC building; IS 1893:2016; IS 16700; IS 456:2000; IS 800:2007; response spectrum; P–Delta; inter-storey drift; storey shear; overturning moment; peak floor acceleration.**

1.INTRODUCTION

Rapid urban densification in Indian metropolitan regions has driven an increasing adoption of mid- to high-rise reinforced concrete buildings in the 50–100 m height range, where lateral performance can govern overall proportioning, detailing, and multidisciplinary coordination. For such buildings, design decisions must balance strength and ductility requirements under earthquake actions with serviceability considerations under wind and everyday occupancy, while ensuring robust stability against second-order effects. Indian design practice anchors these checks in a consistent code framework: IS 1893 (Part 1):2016 for defining seismic actions and analysis procedures, IS 456:2000 for reinforced concrete behavior and detailing, and IS 16700 for tall concrete buildings where both drift and acceleration serviceability are emphasized. Where structural steel elements exist (for example, local framing, embedded steelwork, or connection hardware), IS 800:2007 provides the basis for limit-state design.

The building studied in this paper is a G+18 (19-storey) RC tower with an overall height of 70 m and an average storey height of approximately 3.684 m. The lateral-force-resisting system comprises a central RC core wall system coupled with perimeter RC moment-resisting frames, with rigid floor diaphragm behavior assumed at each storey. This widely used core–frame arrangement is efficient because the core provides significant lateral stiffness and torsional resistance, while the perimeter frames contribute to stiffness distribution, drift profile control, and redundancy. In practice, the stiffness share between core and frames affects where inter-storey drift concentrates, how storey shear is distributed, and how overturning actions are resisted. These response characteristics then drive member sizing decisions (walls, columns, beams), detailing provisions (wall boundaries, coupling beams), and serviceability allowances (cladding joints, elevator tolerances).

Beyond drift and displacement, modern tall-building design increasingly considers peak floor acceleration (PFA) as an indicator for non-structural performance and comfort. Acceleration demands can govern anchorage and bracing of façade systems, partitions, ceilings, mechanical and electrical services, and rooftop equipment, and they can influence occupant perception of motion at upper storeys. IS 16700

International Journal of Engineering Research & Technology (IJERT)
ISSN: 2278-0181
Vol. 15 Issue 04 , April - 2026

specifically recognizes acceleration-related serviceability as part of tall building performance intent. Therefore, the present study is structured around an actionable response set that includes not only displacements and drifts but also storey shears, overturning moments, modal participation, and PFA profiles. The goal is to document an ETABS modeling workflow that yields decision-ready outputs and to interpret those outputs to identify governance (wind vs seismic), drift-critical height bands, and practical optimization pathways.

The remainder of the paper is organized as follows. Section 2 describes the modeling assumptions, material idealizations, and analysis setup adopted in ETABS. Section 3 presents global dynamic characteristics and storey-wise results using the original figures exported from the submitted model data. Section 4 discusses the observed governance split, stiffness distribution implications, P–Delta stability sensitivity, torsional behavior, and non-structural considerations. Section 5 concludes with key findings and targeted recommendations for subsequent design iterations and coordination.

2. METHODOLOGY

2.1 Code basis and performance intent. Seismic actions are defined using IS 1893 (Part 1):2016, which provides the response spectrum form, zoning and importance parameters, and analysis procedures for buildings. The tall-building performance perspective is aligned with IS 16700, which applies to reinforced concrete buildings with heights greater than 50 m and emphasizes both structural safety and serviceability (including drift and acceleration-related checks). Reinforced concrete section behavior, detailing philosophy, and material requirements are taken consistent with IS 456:2000. In addition, IS 800:2007 is referenced where steel components or connections are present or where steel design principles are required for ancillary elements. The objective is not to reproduce full code calculations in this paper, but to ensure that the modeling and response extraction align with the intent and the typical checks implied by these Indian standards.

2.2 Geometry, structural system, and boundary conditions. The building comprises 19 storeys (G+18) with a total height of 70 m. A rigid diaphragm is assigned at every storey, ensuring that lateral inertial forces are distributed to the vertical lateral system in proportion to in-plane stiffness and connectivity. The vertical lateral system is a coupled arrangement of central RC core walls and perimeter RC frames. Supports are modeled as fixed at the base, representing a stiff foundation idealization; base reactions extracted from analysis thus represent actions transferred to the foundation level.

2.3 Material modeling and stiffness modifiers. Reinforced concrete frames and walls are modeled with cracked-section stiffness modifiers to better represent in-service stiffness under sustained gravity and lateral actions. This practice is consistent with the recognition in tall-building design that elastic analyses should reflect realistic stiffness so that computed drift and acceleration demands are not unconservatively low. Slabs are meshed as required for force transfer, and diaphragm action is enforced by rigid diaphragm assignment.

2.4 Mass source, damping, and P–Delta. The mass source is defined from permanent loads together with an appropriate fraction of live load, consistent with standard seismic mass definitions. Classical (modal) damping is used, consistent with common building analysis practice. P–Delta effects are enabled for lateral load cases to capture second-order amplification of drifts and member actions. This is particularly important in tall buildings where stability sensitivity may increase as stiffness distribution and gravity load paths evolve during design iterations.

2.5 Load cases and analysis types. Seismic demand is evaluated using response spectrum analysis in both principal directions (EQX and EQY). Along-wind action is evaluated as a serviceability case in the X direction (WindX) based on the project's wind definition; the extracted outputs are used primarily for displacement and acceleration serviceability interpretation. Modal analysis is performed using sufficient modes to achieve high mass participation; in the submitted model results, the first eight modes achieve approximately 95% cumulative modal mass participation, which supports the adequacy of response-spectrum combination.

2.6 Output extraction and plotting. The ETABS output set extracted includes (a) modal periods and participation, (b) storey displacement envelopes, (c) inter-storey drift ratios, (d) storey shear distributions, (e) base overturning moments, and (f) peak floor acceleration profiles. The original plots exported from the model are retained in this paper as Figures 1–5 to ensure fidelity to the submitted data.

Before you begin to format your paper, first write and save the content as a separate text file. Keep your text and graphic files separate until after the text has been formatted and styled. Do not use hard tabs, and limit use of hard returns to only one return at the end of a paragraph. Do not add any kind of pagination anywhere in the paper. Do not number text heads-the template will do that for you.

Finally, complete content and organizational editing before formatting. Please take note of the following items when proofreading spelling and grammar:

3. RESULTS

This section summarizes the global dynamic properties and the storey-wise response quantities extracted from the ETABS model. The presentation emphasizes envelopes and peak values because these directly inform design checks and optimization

International Journal of Engineering Research & Technology (IJERT)
ISSN: 2278-0181
Vol. 15 Issue 04 , April - 2026

decisions. Figures are reproduced from the submitted dataset without alteration.

3.1 Global dynamic characteristics. The extracted modal properties indicate fundamental translational periods of approximately 3.2 s in both principal directions (T1x ≈ 3.2 s and T1y ≈ 3.2 s) and a first torsional period of approximately 1.1 s. Cumulative modal mass participation reaches about 95% within the first eight modes, demonstrating adequate modal completeness for response-spectrum analysis. Figure 1 presents the modal participation mass distribution, showing dominant contribution from the first sway modes and meaningful participation from subsequent modes that influence higher-storey response and acceleration ripples.

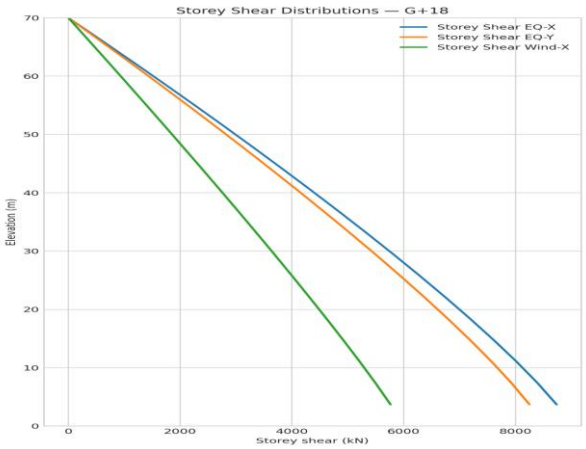

Figure 1. Modal participation mass for the first eight modes (submitted ETABS output).

3.2 Displacement envelopes and governance. Figure 2 shows the height-wise lateral displacement envelopes for EQX, EQY and WindX. The profiles are smooth and consistent with an overall cantilever-like response of a core–frame system, with minor curvature differences attributable to higher-mode contributions. The roof displacement under WindX is the largest, approximately 220 mm, indicating that wind governs roof-level serviceability movement. Under seismic response-spectrum actions, roof displacement is lower, approximately 170 mm for EQX and 160 mm for EQY. This split in governance is important: wind displacement commonly informs façade drift joints, curtain wall anchor allowances, and elevator guide tolerances, whereas seismic displacement must be evaluated in combination with drift limits and ductile detailing requirements.

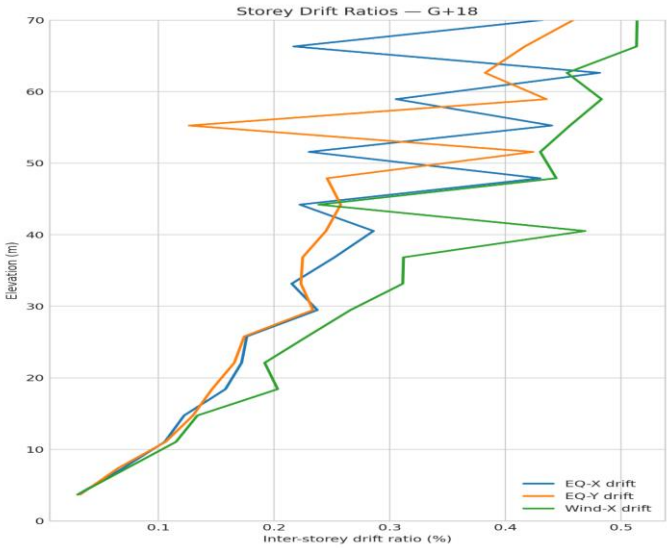

Figure 2. Lateral displacement envelopes for EQX, EQY and WindX over building height (submitted ETABS output).

3.3 Inter-storey drift ratios. Figure 3 plots storey-wise inter-storey drift ratios for EQX, EQY and WindX. Peak drift occurs in an upper-middle height band rather than at the base, which is typical when the stiffness distribution and mode shapes combine to produce a drift concentration away from the lowest storeys. The maximum drift ratio is approximately 0.357% in EQX and 0.342% in EQY, while WindX produces a maximum drift ratio of approximately 0.309%. These peak values are below the commonly used drift limits in Indian practice for reinforced concrete buildings (project-specific limits should be confirmed), but the location of the peaks is critical for targeted stiffness tuning. In particular, local core wall thickness adjustments, coupling-beam proportioning, or perimeter frame stiffness enhancement at the drift-critical band can reduce peak drift efficiently without significantly increasing base actions.

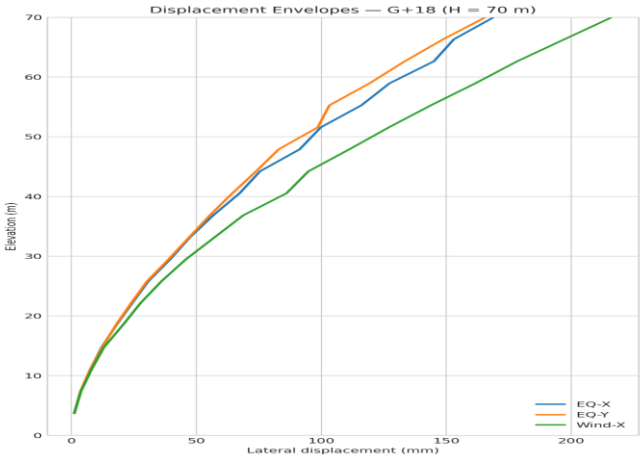

Figure 3. Storey-wise inter-storey drift ratios for EQX, EQY and WindX (submitted ETABS output).

International Journal of Engineering Research & Technology (IJERT)
ISSN: 2278-0181
Vol. 15 Issue 04 , April - 2026

3.4 Storey shear and overturning moment. Storey shear distributions (Figure 4) exhibit the expected near-triangular trend with maximum shear at the base and reducing towards the roof. The approximate base shear values extracted are about 9,000 kN for EQX, 8,500 kN for EQY, and 6,000 kN for WindX. The corresponding base overturning moments are approximately 267,000 kN·m (267 MN·m) for EQX, 252,000 kN·m (252 MN·m) for EQY, and 188,000 kN·m (188 MN·m) for WindX. Directional differences reflect variations in lateral stiffness and mass distribution between the principal axes. These base actions provide the primary inputs for foundation design and for verifying global stability and load path continuity, while the storey shear profile informs storey-level collector demands and wall/frame force distribution.

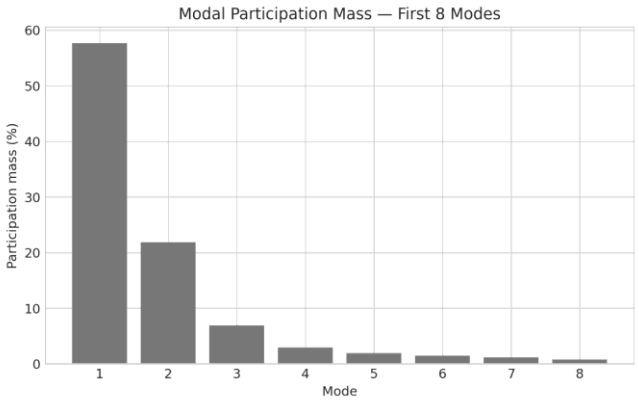

Figure 4. Storey shear distributions (submitted ETABS output).

3.5 Peak floor acceleration (PFA). Figure 5 shows PFA profiles expressed in g along the height of the building. The profiles generally increase with elevation, which is expected because upper storeys experience greater dynamic amplification and reduced effective stiffness. Minor ripples are present, indicating higher-mode participation, consistent with the modal participation distribution. Seismic PFA approaches about 0.12 g at the roof, while wind PFA is around 0.05 g. These results are significant for non-structural design: acceleration-sensitive components such as façade panels, ceiling systems, suspended services, equipment supports, and rooftop installations must be detailed for these acceleration demands. In addition, acceleration response can influence occupant comfort, and tall-building guidelines often emphasize controlling wind-induced accelerations for habitability.

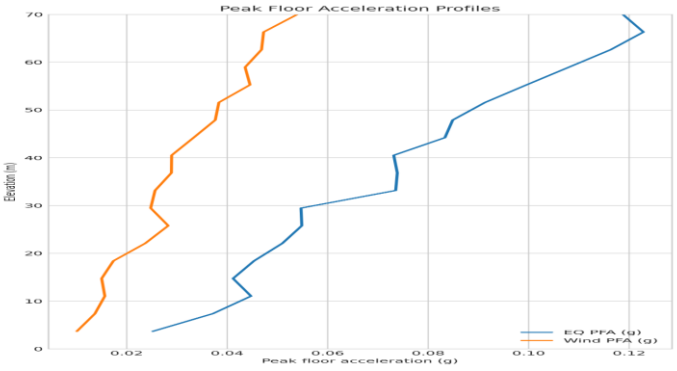

Figure 5. Peak floor acceleration (PFA) profiles in g (submitted ETABS output).

4. DISCUSSION

4.1 Governance split and design implications. The extracted responses demonstrate a clear split between serviceability governance and strength/ductility governance. WindX governs roof displacement (about 220 mm) and contributes meaningfully to roof-level accelerations, which are often the controlling criteria for façade movement allowances and comfort-related assessments. In contrast, seismic response-spectrum actions govern peak drift, with maximum drift ratios near 0.357% (EQX) and 0.342% (EQY). This split suggests that design optimization should treat wind and seismic objectives separately: wind-driven refinement may focus on roof displacement and acceleration control (for example, through stiffness enhancement or damping strategies), while seismic-driven refinement may focus on drift concentration zones and ductile detailing of energy-dissipating components.

4.2 Stiffness distribution and drift-shape interpretation. The drift profiles show peaks in the upper-middle storeys, indicating that stiffness is not uniformly distributed in a way that produces a perfectly linear drift gradient. In core–frame systems, the core typically provides the majority of lateral stiffness, and the perimeter frames act to reduce drift concentration and improve redundancy. When drift peaks occur away from the base, it often indicates either a relative stiffness reduction at certain heights (for example, changes in wall thickness, openings, transfer levels, or architectural constraints) or the influence of higher modes that shape curvature. A pragmatic tuning approach is therefore to add stiffness locally where drift peaks, such as by modestly increasing core wall thickness or strengthening coupling beams at the drift-critical band, or by increasing perimeter frame participation through spandrel depth or beam–column stiffness ratios at selected storeys. Uniform stiffening across the full height is generally less efficient and may undesirably increase base actions.

4.3 P–Delta and stability sensitivity. P–Delta effects were enabled in the analysis, which is appropriate for a 70 m building

International Journal of Engineering Research & Technology (IJERT)
ISSN: 2278-0181
Vol. 15 Issue 04 , April - 2026

where second-order effects can influence drift and member demand, especially as design iterations alter column sizes and axial loads. At the reported peak drift levels (≤ about 0.36%), second-order amplifications are relevant but appear controlled. Nevertheless, stability indices and drift amplification factors should continue to be monitored in subsequent iterations, particularly if architectural changes introduce soft-storey tendencies or if stiffness reductions occur at mechanical levels. Maintaining P–Delta in the analysis also helps ensure that drift-based serviceability checks remain realistic.

4.4 Torsional behavior and diaphragm action. The first torsional period is about 1.1 s, and the absence of pronounced torsional amplification in the presented storey-wise response plots suggests that the plan is reasonably regular and that rigid diaphragm behavior provides effective in-plane distribution. However, torsional checks should still be performed using accidental eccentricity and code-recommended combinations because even small plan irregularities or stiffness asymmetries can produce localized edge drift demands that affect façade and partition performance. Attention is warranted at levels with stiffness discontinuities, such as mechanical floors, podium transfers, or setbacks.

4.5 Non-structural performance and acceleration-sensitive coordination. The PFA results provide a direct bridge between structural analysis and multidisciplinary design. Roof-level seismic PFA approaching 0.12 g and wind PFA around 0.05 g imply meaningful demands on anchors and bracing of non-structural systems. For façade design, both displacement compatibility (from Figure 2) and acceleration demand (from Figure 5) are relevant: displacement governs joint widths and movement accommodation, while acceleration governs inertia forces on panels and fixings. For MEP systems, acceleration governs hanger and brace forces and can affect equipment isolation. Consequently, the extracted response set should be shared with façade and MEP teams early, and non-structural detailing should be reviewed in zones where drift peaks or acceleration increases rapidly.

4.6 Limitations and next steps. The present paper documents a single ETABS-based linear dynamic analysis with cracked stiffness modifiers and P–Delta. As the design progresses, it may be appropriate to supplement the study with sensitivity analyses on stiffness modifiers, mass source assumptions, and diaphragm idealization, as well as refined wind evaluation consistent with the selected wind code basis and local terrain/exposure. If the building is categorized as tall or important, additional checks aligned with the latest IS 16700 provisions may include explicit comfort evaluation under wind and verification of robustness and progressive collapse considerations. Finally, once member sizing is closer to final, a detailed design stage should verify that local element demands and detailing requirements are satisfied under governing load combinations and that drift and acceleration criteria remain within project-defined targets.

5. CONCLUSION

This paper presented a ETABS modeling workflow and response synthesis for a 70 m (G+18) reinforced concrete building with a central core and perimeter moment-resisting frames, framed within an Indian Standards perspective (IS 1893:2016 for seismic action, IS 16700 for tall-building performance intent, IS 456 for RC behavior and detailing, and IS 800 where steel design basis is relevant). The dynamic characteristics show fundamental translational periods of about 3.2 s and a first torsional period of about 1.1 s, with approximately 95% modal mass participation achieved in the first eight modes, supporting the adequacy of the response-spectrum procedure.

A clear governance split was observed. Wind governs roof displacement (about 220 mm) and contributes to roof-level accelerations relevant to comfort and non-structural systems, while seismic actions govern peak inter-storey drift (about 0.357% in EQX and 0.342% in EQY). Storey shear and overturning responses are consistent with expected behavior of a core–frame system at this height, with base shear approximately 9,000 kN in EQX and base overturning moment approximately 267 MN·m. Peak floor acceleration increases with height and approaches about 0.12 g at the roof under seismic action, reinforcing the need to coordinate acceleration demands with façade and services design.

Based on the response patterns, the following recommendations are made for subsequent design iterations: (i) apply targeted stiffness tuning at the drift-critical upper-middle storey band rather than uniform stiffening, (ii) retain P–Delta effects and monitor stability indices as member sizes and gravity loads evolve, (iii) maintain torsional checks with accidental eccentricity, especially at any stiffness discontinuities, and (iv) share displacement, drift, and PFA profiles with non-structural designers to ensure adequate movement allowances and anchorage/bracing design. The response set and the preserved figures provide a decision-ready basis for optimizing structural performance, constructability, and multidisciplinary coordination.

REFERENCES

*Codes, standards, and software manuals

[1] Bureau of Indian Standards (BIS). IS 1893 (Part 1):2016, Criteria for Earthquake Resistant Design of Structures – Part 1: General Provisions and Buildings. Public access copy: https://archive.org/details/gov.in.is.1893.1.2016

[2] National Information Centre of Earthquake Engineering (NICEE). IITGN–World Bank Project resources and commentary related to IS 1893:2016. https://www.nicee.org/IITGN-WB_Codes.php

International Journal of Engineering Research & Technology (IJERT)
ISSN: 2278-0181
Vol. 15 Issue 04 , April - 2026

[3] Bureau of Indian Standards (BIS). IS 16700:2023, Criteria for Structural Safety of Tall Concrete Buildings (First Revision). Public access copy: https://archive.org/details/gov.in.is.16700.2023

[4] Bureau of Indian Standards (BIS). IS 456:2000, Plain and Reinforced Concrete – Code of Practice. Public access copy: https://law.resource.org/pub/in/bis/S03/is.456.2000.pdf

[5] Bureau of Indian Standards (BIS). IS 800:2007, General Construction in Steel – Code of Practice. Public access copy: https://dn790009.ca.archive.org/0/items/gov.in.is.800.2007/is.800.2007.pdf

[6] Bureau of Indian Standards (BIS). IS 875 (Part 1):1987 Dead Loads. Public access copy: https://law.resource.org/pub/in/bis/S03/is.875.1.1987.pdf

[7] Bureau of Indian Standards (BIS). IS 875 (Part 2):1987 Imposed Loads. Public access copy: https://law.resource.org/pub/in/bis/S03/is.875.2.1987.pdf

[8] Bureau of Indian Standards (BIS). IS 875 (Part 3):2015 Wind Loads (with Amendment 2016). Public access copy: https://archive.org/details/gov.in.is.875.3.2015

[9] Bureau of Indian Standards (BIS). IS 13920:2016 Ductile Design and Detailing of Reinforced Concrete Structures Subjected to Seismic Forces. Public access copy: https://archive.org/details/gov.in.is.13920.2016

[10] Bureau of Indian Standards (BIS). National Building Code of India 2016 (NBC 2016), Volume 1. Public access copy: https://archive.org/details/nationalbuilding01

[11] Computers and Structures, Inc. ETABS® User's Guide – Integrated Building Design Software. https://docs.csiamerica.com/manuals/etabs/User's%20Guide.pdf

[12] CSI Knowledge Base. CSI Analysis Reference Manual – Documentation page. https://wikicsiamerica.atlassian.net/wiki/spaces/doc/pages/1245505/CSI+Analysis+Reference+Manual

*Research papers and technical reports:

[13] Değer, Z. T., Yang, T. Y., Wallace, J. W., and Moehle, J. (2014). "Seismic performance of reinforced concrete core wall buildings with and without moment resisting frames." The Structural Design of Tall and Special Buildings, 23(9), 663–681.

[14] Godínez, S. E., Álvarez, R., and Restrepo, J. I. (2024). "Nonlinear dynamic seismic analysis of a high-rise concrete core wall building with podiums using the beam-truss model." Bulletin of Earthquake Engineering (Springer).

[15] Ujwal, M. S., Shekar, N. C. Sanjay Shekar, Arya Prathap, C. B. R. Ranjan Gowda, N. Vibhashree, M. Karthik and G. Shiva Kumar (2026). "Influence of soft storeys, facade components, and shear walls on the seismic behavior of high-rise RC buildings." Asian Journal of Civil Engineering (Springer).

[16] Banazadeh, M. (2022). "Seismic performance assessment of high-rise steel moment frame building with reinforced concrete (RC) core wall based on nonlinear time history analysis." Research, Society and Development, 11(4).

[17] Sullivan, T. J., Pham, T. H., and Calvi, G. M. (2008). "P-Delta effects on tall RC frame-wall buildings." Proceedings of the 14th World Conference on Earthquake Engineering (14WCEE), Beijing.

[18] Paulay, T. (1978). "A consideration of P-Δ effects in ductile reinforced concrete frames." Bulletin of the New Zealand National Society for Earthquake Engineering, 11(3), 151–160.

[19] Anajafi, H., and Medina, R. A. (2018). "Evaluation of ASCE 7 equations for designing acceleration-sensitive nonstructural components using data from instrumented buildings." Earthquake Engineering & Structural Dynamics, 47(4), 1075–1094.

[20] González, I., Silva, A., Macedo, L., Monteiro, R., and Castro, J. M. (2019). "Critical assessment of estimation procedures for floor acceleration demands in steel moment-resisting frames." Frontiers in Built Environment, 5, 139.

[21] Liu, R., Bai, W., Dai, J., Shao, Z., Jiang, T., and Zhao, B. (2025). "Research on the design floor response spectrum of buildings by dynamic analysis." Earthquake Engineering and Engineering Vibration, 24, 413–436.

[22] Pozzi, M., and Der Kiureghian, A. (2012). "Response spectrum analysis for floor acceleration." Proceedings of the 15th World Conference on Earthquake Engineering (15WCEE), Lisbon.

[23] Vukobratović, V., and Ruggieri, S. (2021). "Floor acceleration demands in a twelve-storey RC shear wall building." Buildings, 11(2), 38.

[24] Cao, Y., Huang, Y., and Qu, Z. (2021). "Response spectrum analysis of peak floor accelerations of buildings under earthquakes." Journal of Earthquake Engineering. https://doi.org/10.1080/13632469.2021.1961942

[25] Taghavi, S., and Miranda, E. (2003). Response Assessment of Nonstructural Building Elements. PEER Report 2003/05, Pacific Earthquake Engineering Research Center, University of California, Berkeley.

[26] Filiatrault, A., and Sullivan, T. J. (2014). "Performance-based seismic design of nonstructural building components: The next frontier of earthquake engineering." Earthquake Engineering and Engineering Vibration, 13, 17–46.

[27] Taghavi, S., and Miranda, E. (2004). "Estimation of seismic acceleration demands in building components." Proceedings of the 13th World Conference on Earthquake Engineering (13WCEE), Vancouver.

[28] Rodriguez, M. E., Restrepo, J. I., and Blandón, J. J. (2007). "Seismic design forces for rigid floor diaphragms in precast concrete building structures." Journal of Structural Engineering (ASCE), 133(11), 1604–1615.

[29] Tallin, A., and Ellingwood, B. (1985). "Wind-induced motion of tall buildings." Engineering Structures, 7(2). https://doi.org/10.1016/0141-0296(85)90004-5

[30] Abu-Zidan, Y., Mendis, P., Gunawardena, T., Mohotti, D., and Fernando, S. (2022). "Wind design of tall buildings: The state of the art." Electronic Journal of Structural Engineering, 22(1).

[31] Burton, M. D., Kwok, K. C. S., and Abdelrazaq, A. (2015). "Wind-induced motion of tall buildings: Designing for occupant comfort." International Journal of High-Rise Buildings, 4(1), 1–8.

[32] Kareem, A., Kijewski, T., and Tamura, Y. (1999). "Mitigation of motions of tall buildings with specific examples of recent applications." Wind and Structures, 2(3), 201–251.

[33] Gora, A., Huang, M., Wang, C., and Zhang, R. (2025). "Wind-induced dynamic performance evaluation of tall buildings considering future wind climate." Applied Sciences, 15(9), 5073. https://doi.org/10.3390/app15095073

[34] Li, Q. S. (2008). "Evaluation of wind-induced vibration of tall buildings and reliability analysis: A case study." Journal of Wind Engineering and Industrial Aerodynamics.

[35] Bonati, A., Caterino, N., Cimmino, M., Coppola, O., De Angelis, A., Maddaloni, G., and Occhiuzzi, A. (2025). "Assessment of seismic capacity of building envelope nonstructural components." Journal of Earthquake Engineering. https://doi.org/10.1080/13632469.2025.2470328

[36] Puthanpurayil, A. M., Carr, A. J., Jury, R., and Wood, D. (2019). "A simplified peak floor acceleration estimation for existing buildings: A response history-based method." Proceedings of the SESOC/NZSEE Conference.